Abstract # 1167, Oral 7A-1, Thursday 6/23 at 9:30am, can be up to eight pages THIS IS INVITED SAND2011-3999C

IMPACT OF TIME VARYING LOADS ON THE PROGRAMMABLE PULSED POWER DRIVER CALLED GENESIS *

S.F. Glover[1ξ], J.-P. Davis[1], L.X. Schneider[1], K.W. Reed[1], G.E. Pena[1], C.A. Hall[1], H.L. Hanshaw[1], R.J. Hickman[1], K.C. Hodge[2], R.W. Lemke[1], J.M. Lehr[1], D.J. Lucero[2], D.H. McDaniel[1], J. G. Puissant[2], J.M. Rudys[1], M.E. Sceiford[1], S.J. Tullar[2], D.M. Van De Valde[3], F.E. White[2], L. K. Warne[1], R. S. Coats[1], R. E. Jorgenson[1], W. A. Johnson[1]

[1]*Sandia National Laboratories, Albuquerque, NM 87185 USA*
[2]*Ktech Corporation, Albuquerque, NM. 87123 USA*
[3]*EG&G, Albuquerque, NM 87107 USA*

Abstract

The success of dynamic materials properties research at Sandia National Laboratories has led to research into ultra-low impedance, compact pulsed power systems capable of multi-MA shaped current pulses with rise times ranging from 220-500 ns. The Genesis design consists of two hundred and forty 200 kV, 60 kA modules connected in parallel to a solid dielectric disk transmission line and is capable of producing 350 kbar of magnetic pressure in a 1.75 nH, 20 mm wide strip line load. Strip line loads operating under these conditions expand during the experiment resulting in a time varying load that can impact the performance and lifetime of the system. This paper provides analysis of time varying strip line loads and the impact of these loads on system performance. Further, an approach to reduce dielectric stress levels through active damping is presented as a means to increase system reliability and lifetime.

I. INTRODUCTION

The goal of Genesis R&D is to create a technology base that enables the design of highly compact multi-MA current platforms with precision pulse shaping capabilities. Genesis technology development is directed at applications where physical footprint constraints are present and/or a high degree of pulse shaping is required. Genesis capabilities are consistent with the operating envelope required for a magnetic compression driver for dynamic materials experiments located at a synchrotron light source to enable time-resolved x-ray diffraction and imaging measurements.

The Genesis project has explored modular system architectures operating at aggressively high electric field values. This enables ultra-low inductance topologies which greatly reduces the system's operating voltage requirements when driving low impedance loads. The highly modular nature enables precision pulse shaping through the use of genetic optimization techniques to select trigger points for individual modules. Genetic optimization also enables the minimization of peak voltage variations throughout the system which are created by the temporal triggering of the tightly coupled pulse forming.

Performance of a system like Genesis can be significantly impacted by the load characteristic due to the tight coupling between the pulsed forming components and the load. The tight coupling is a result of the extremely low inductance, solid dielectric feed structure. This paper will explore the response of the Genesis architecture to a time varying load and means to control the performance of this system through optimized triggering of the high current modules.

II. GENESIS SYSTEM

The multimodule Genesis system and its disk transmission line structure are depicted in Figure 1 and Figure 2. Modules contain the initial energy store and switches that are used to switch module current into the disk transmission line. The transmission line plates provide an ultra-low impedance path from the parallel modules to the load through the use of a solid dielectric insulation system. Precision pulse shapes are achieved through temporal triggering of 240 high current modules to drive a pressure wave into material samples for dynamic materials experiments. Genesis was designed to produce waveforms up to 5 MA peak current which develops peak magnetic pressures of 250-350 kbar in a 20 mm wide, strip line load. A custom load assembly was designed to interface to the solid dielectric insulated disk plate structure at the center of the driver. The load inductance was determined through static analysis [1]. Use of solid dielectric insulation begins in the base of the high voltage modules and continues through the disk transmission line to a solid dielectric insulated strip line load. High inductance insulator stacks are not required in the Genesis design as there is no need to separate fluids or a fluid from a vacuum region as is typically found in conventional pulsed forming technologies including Linear Transformer Drivers (LTDs).

* Sandia National Laboratories is a multi-program laboratory managed and operated by Sandia Corporation, a wholly owned subsidiary of Lockheed Martin Corporation, for the U.S. Department of Energy's National Nuclear Security Administration under contract DE-AC04-94AL85000.
ξ email: sfglove@sandia.gov

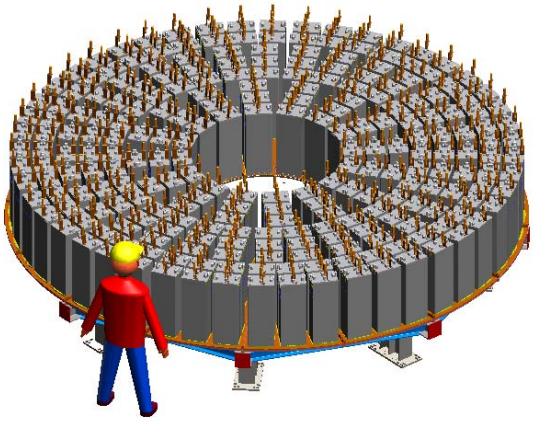

Figure 1. Solidworks model of Genesis, a 240 module high current driver.

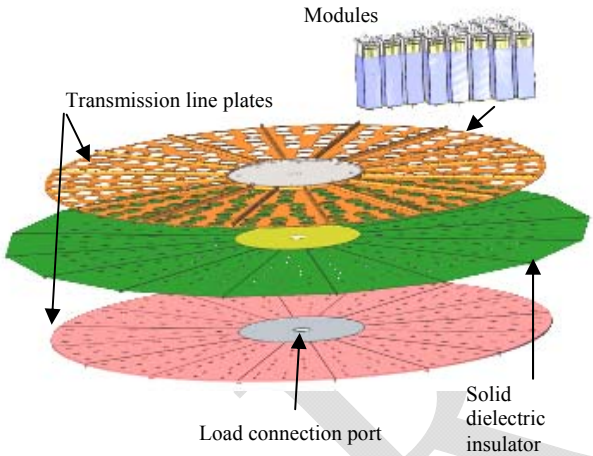

Figure 2. Genesis system components including high voltage modules and a solid dielectric insulated disk transmission line structure.

The disk transmission line consists of sixteen wedge shaped plates and a circular center section. The plates contain 240 ports that allow for module connection and removal for maintenance. Fifteen of the modules are included in the figure. The gap separating the disk transmission line plates was minimized to reduce circuit inductance, module charge voltage requirements and system size. This is achieved through the use of a solid dielectric insulation system operating at an average pulsed field of 630 kV/cm (is this zero to peak??). The strip line load, shown in Figure 3, is pre-mounted to interface hardware and installed in the center of the driver as indicated in Figure 2. The inductance of this load out to a 5.2 cm radius is 1.75 nH.

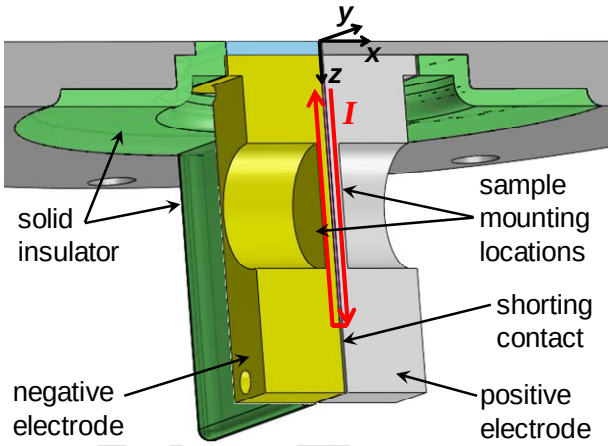

Figure 3. Isometric view from bottom of stripline load with counter-bores for mounting samples, indicating current path and coordinates referenced in Section III.

Figure 4 shows a cutaway view of a high current module which includes the outer housing, cabling, and gas lines. Each module contains two 80 nF capacitors, a High Current Electronics Institute (HCEI) switch [2] [3] [4], trigger resistor, and charge resistors. The capacitors and switch are arranged in the form of a two stage Marx Generator that can be charged to ±100 kV. One capacitor is connected electrically to the bottom of the module, the other to an electrode that protrudes out the bottom of the module. This electrode penetrates the solid insulator between the transmission line plates making electrical connection to the bottom transmission line plate.

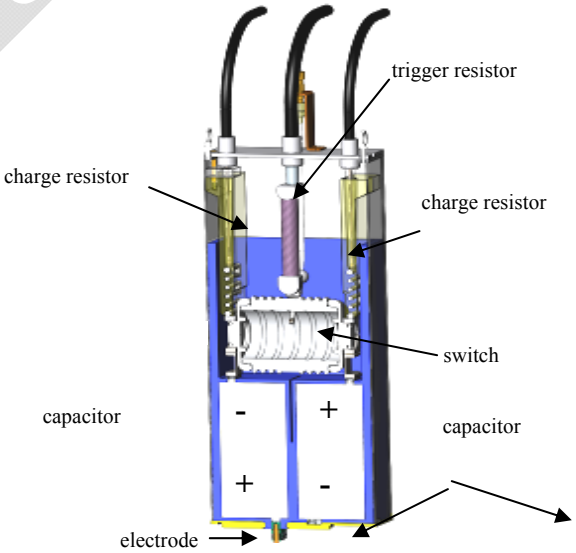

Figure 4. Module cutaway. The blue region is solid dielectric, allowing a more compact configuration.

A state equation based circuit model of the system shown in Figure 1 has been created in MATLAB [5] to

model system performance during pulse shaping. One sixteenth of the circuit diagram (one wedge of the transmission line plates) is depicted in Figure 5. The complete circuit diagram is circular in shape. This model represents each module as an RLC circuit with an ideal switch. Inclusion of disk transmission line elements allows for the geometrical location of modules relative to each other and connection to the load at the center of the 2-D circuit model.

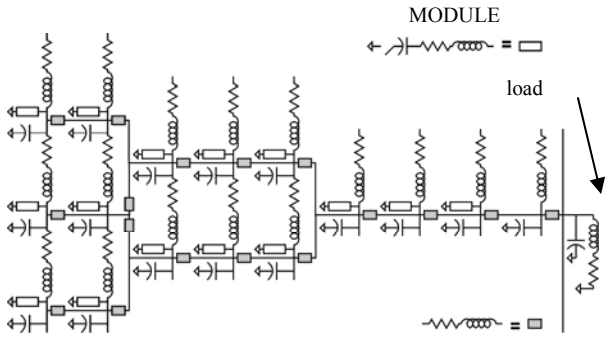

Figure 5. One sixteenth of the Genesis circuit diagram.

A genetic algorithm was used to determine optimum trigger times to produce precision waveshapes for various dynamic materials experiments. This approach has been previously demonstrated [6] using the Genetic Optimization System Engineering Tool [7]. Current shapes plotted in Figure 6 indicate both the range and flexibility of Genesis to produce dynamic current pulses. Other waveshapes are possible, including flat top pulses and modified fall times.

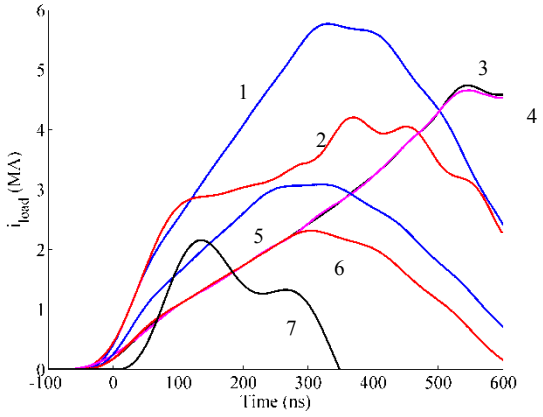

Figure 6. Example output pulse shapes for various materials. 1) Tungsten – 5.7 MA 2) Iron - 4 MA 3) Polypropylene – 4.7 MA 4) Polypropylene- 4.7 MA 5) Tungsten - 3 MA 6) Tungsten - 2 MA 7) 28 modules at t=0.

The simulations included in Figure 6 were previously based on simulations using a fixed load inductance [6] [8]. This earlier modeling did not account for movement of the strip line load during the primary pulse due to the high magnetic pressure at these current levels. It is this effect that allows energy from the current to be transmitted in the form of pressure to a material sample located on the outside surface of the strip line electrodes. Movement of the strip line time results in a time varying load impedance that impacts the performance of Genesis. The following sections discuss the analysis of the time varying load and the impact on system performance.

III. TIME VARYING LOADS

The prototypical Genesis stripline load for dynamic materials studies consists of two parallel plate electrodes separated 432 μm by layers of Kapton® polyimide film and shorted at one end. The stripline configuration shown in Figure 3 is 20 mm wide, 50 mm long, and 10 mm thick, with a counter-bore machined in the back side down to 1-2 mm remaining thickness where material samples are mounted. The pulse of current flowing along the inner surfaces of the stripline (toward and away from the shorting contact) generates a time-varying magnetic field between the plates. As depicted in Figure 7, the resulting $\boldsymbol{J}\times\boldsymbol{B}$ Lorentz force manifests as a time-varying magnetic pressure on the material in the electrodes, resulting in a planar, time-ramped wave of mechanical stress propagating from the electrode into the sample material. The electrode material is Joule heated to gas and plasma states by the high current density, lowering its conductivity and allowing the magnetic field to diffuse into the electrode. The magnetic diffusion front propagates more slowly than the mechanical stress wave, allowing material dynamics experiments on the evolution of the mechanical stress wave in the sample material that are decoupled from MHD effects in the electrode.

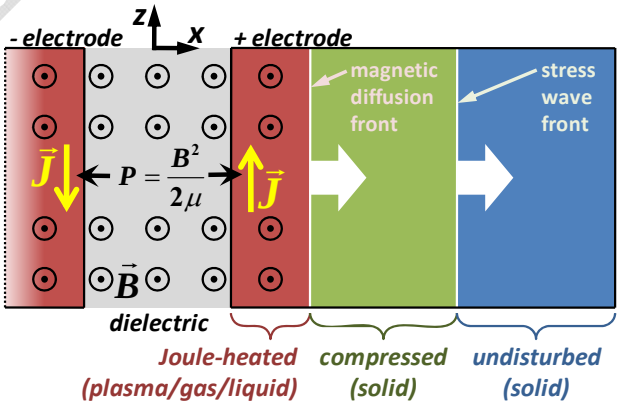

Figure 7. Schematic in *x*-*z* plane (*c.f.* Figure 3) to illustrate generation of a mechanical stress wave and magnetic diffusion front in stripline electrodes. $\boldsymbol{J}$ is current density, $\boldsymbol{B}$ is magnetic field, P is magnetic pressure, and μ is permeability.

The electrical properties of the stripline load as seen by the rest of the machine vary in time as the magnetic field topology varies in time due to (1) acceleration of the

electrodes away from each other by the magnetic pressure and (2) diffusion of the magnetic field into the electrodes. Computation of time-dependent magnetic-field topology requires magneto-hydrodynamics (MHD) simulations of the stripline during the current pulse. Though inherently a 3-D problem due to the stripline's finite length, stripline properties are reasonably well represented by a 2-D problem in the transverse plane (*x*-*y* plane in Figure 3) that cuts the stripline halfway along its length.

A 2-D simulation was performed using the finite-difference Alegra MHD code [9] with an experimental configuration relevant to a 5-MA peak current version of the tungsten waveform #1 in Figure 6. This consisted of 1.5-mm thick samples of tungsten mounted on aluminum electrodes in counter-bores of 1.0 mm remaining floor thickness. Though real experiments typically use a different thickness sample or no sample on the opposite electrode, the present simulations used a symmetric stripline to simplify the problem. The simulation domain is semi-circular with the straight edge on the *x*-axis symmetry line, and includes both electrodes and surrounding vacuum region to ~7 cm radius. Figure 8(a) shows only that portion of the domain closest to the stripline, at a time t = 250 ns, which is the time of peak applied current (see Figure 9).

While the Genesis load has solid dielectric between the electrodes, the present calculations instead use a vacuum gap because wide-ranging equation-of-state (EOS) and conductivity models (encompassing states from solid through plasma and under compression) were not available for dielectric materials. The error due to this substitution is expected to be small and dominated by a hydrodynamic perturbation from thermal expansion of the dielectric material. Quantifying the error will require further work. Aside from the dielectric issue, we have high confidence in the MHD simulation results because they rely on wide-ranging EOS and conductivity models for aluminum of high demonstrated accuracy [10].

A 2-D MHD simulation driven by a prescribed load current $I(t)$ perpendicular to the plane of the mesh, as in Figure 8(a), can provide an accurate inductance history $L(t)$ by integrating the magnetic field energy in the mesh:

$$L(t) = \frac{h}{\mu_0 \, I(t)^2} \int |\boldsymbol{B}(t)|^2 \, dx \, dy$$

where h is the height of the stripline up to the shorting contact, and the vacuum permeability $\mu_0 \approx \mu$ for non-magnetic materials. The singularity as $I \rightarrow 0$ at a current reversal, however, means this approach is not useful for determining load inductance during late-time ringing of Genesis. In fact, any method of obtaining inductance from electrical properties of the MHD mesh will fail for the same reason.

An alternative, approximate approach to compute $L(t)$ is to first extract from the MHD solution at each time of interest the geometry of an equivalent perfect-electrical-conductor (PEC) stripline that has the same B-field at the gap centerline, then compute a 2-D electrostatic solution of the PEC stripline with the electrodes at ±0.5 V, and finally use the traveling electro-magnetic (TEM) wave approximation to obtain inductance per unit length L_ℓ by integrating the electric field energy as follows:

$$L_\ell = \left(\varepsilon_0 c_0^2 \int |\boldsymbol{E}|^2 \, dx \, dy \right)^{-1}$$

where

The use of 1-D MHD simulations allows simple algorithms for determining equivalent geometry as a function of the initial stripline cross-section geometry (electrode width, electrode thickness, and separation) and an equivalent anode-cathode (A-K) gap that accounts for material motion and B-field diffusion, though this introduces additional approximations by neglecting the 2-D topology of motion and diffusion at the lateral edges.

The 1-D problem is represented by a 2-D MHD computation on a mesh in the longitudinal plane (*x*-*z* plane in Figure 3) that is one cell wide and defines a line through the thickness of the electrode and sample at the center of the counter-bore.

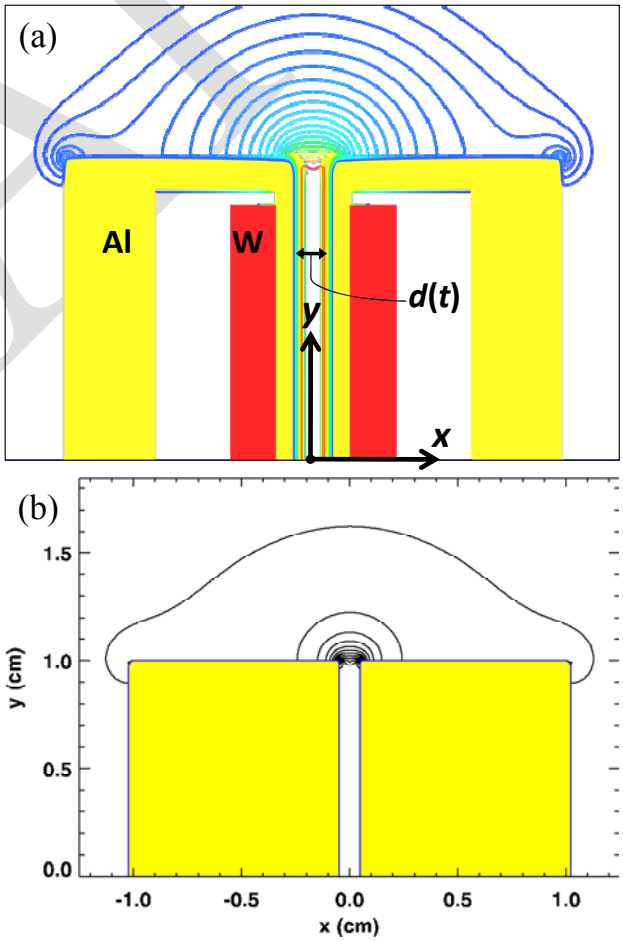

Figure 8. (a) 2-D MHD result at t = 250 ns with line contours of B-field and filled contours of density (both on log scale) showing equivalent gap $d = 2x_{PEC}$; (b) 2-D static

result at t = 250 ns for equivalent PEC stripline with d = 0.987 mm and linear-scale line contours of B-field.

Equivalent A-K gap can be computed at each time by simply integrating the B-field in the 1-D MHD solution:

$$x_{\mathrm{PEC}} = x_0 + \frac{1}{B_z(x_0)} \int_{x_0}^{x_1} B_z(x)\, dx$$

where the A-K gap centerline is at x = 0, the gap-facing and outward-facing electrode material boundaries are at x_0 and x_1, respectively, and the gap-facing boundary of the equivalent PEC is at x_{PEC}. This formulation also fails as $B_z(x_0) \rightarrow 0$ at current reversal, thus we instead used the following formulation that tracks the position of the initial magnetic diffusion front while ensuring a monotonic increase of separation in the equivalent PEC geometry:

$$x_{\mathrm{PEC}} = x_{B\max} + \frac{1}{B_{\max}(x_{B\max})} \int_{x_{B\max}}^{x_1} B_z(x)\, dx$$

where $x_{B\max}$ is the non-decreasing position of the local maximum in B-field corresponding to the initial diffusion front. Figure 9 compares this approach to the 2-D MHD result; inductance of the latter shoots up due to the singularity near 500 ns, while the alternative approach, while matching the 2-D result rather well at earlier times, shows inductance flattening out as the diffusion front slows down.

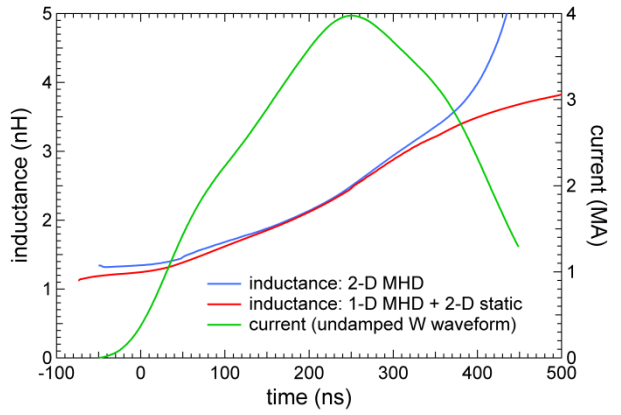

Figure 9 Comparison of $L(t)$ during initial pulse computed using the 2-D MHD and the approximate (1-D MHD + 2-D electrostatic) approaches.

The above calculation neglects coupling between the machine and the load; the inductance of the load seen by the machine affects the current delivered to the load by the machine. Since including the circuit model of Genesis in the Alegra simulation would be non-trivial, this coupling is addressed by iteration.

IV. TIME VARYING LOAD IMPACT

Implementing the time varying load in the Genesis simulation was achieved by creating a lookup table of inductances versus time for a given load current. The challenge with this approach is that if the new load currents do not match the currents used to generate the time varying inductance then the inductance calculations will be incorrect. The flexibility of Genesis pulse shaping helps eliminates this problem by changing trigger times to ensure that the new load current matches the current used to create the lookup table. With this in mind the steps to determine required switch trigger times with a time varying load becomes:

- Create an ideal current pulse shape that pressurizes a material sample along an isentrope.
- Run an optimization on the Genesis circuit model with static load impedance, seeking an optimal match between the ideal pulse shape and the simulated pulse shape.
- Determine the dynamic load inductance using 1-D MHD with 2-D static analysis and the simulated current.
- Run the optimization again on the Genesis model, with a dynamic load inductance fitting the pulse to the shape achieved in the second bullet above.

Ideal load current shapes for isentropic compression can be a range of forms as indicated in Figure 6. In the examples that follow we have chosen to look at two extremes from that set. One with a short rise time (Tungsten - W) and one with a long rise time (Polypropylene – PP). Figure 10 contains simulated examples of waveforms for each material type utilizing a fixed load inductance. The ideal waveforms were created for these materials to move them along an isentrope but are ideal in the sense that they are the shapes that we are trying to achieve and they neglect MHD effects. The ideal waveforms are plotted as red dashed lines that go from zero to the peak. Blue traces are genetically optimized simulated results that seek a best fit to the ideal current while simultaneously seeking a solution that reduces late time reversal of voltage and current (active damping). Green traces are simulated waveforms that do not attempt to minimize reversal. The fit to the ideal current is only lacking near t=0 where the di/dt requirements are limited by the impedances of the system. The number of modules used to achieve each waveform is different: undamped W – 108, damped W – 172, undamped PP - 196, damped PP - 208.

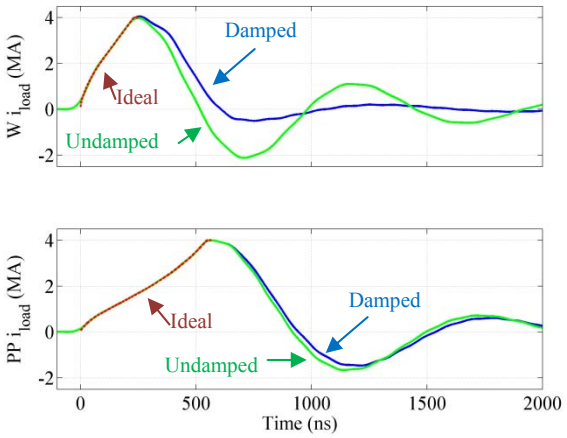

Figure 10. Load currents with fixed load inductance.

Active damping can be effective as indicated in Figure 10 and in Figure 11. Both current reversal and late time oscillations can be reduced which allows for a greater range of pressure characteristics for material science research. Reduction of the electric fields in the transmission line plates as seen in Figure 11 effectively reduces the stress on the dielectrics improving reliability and lifetime.

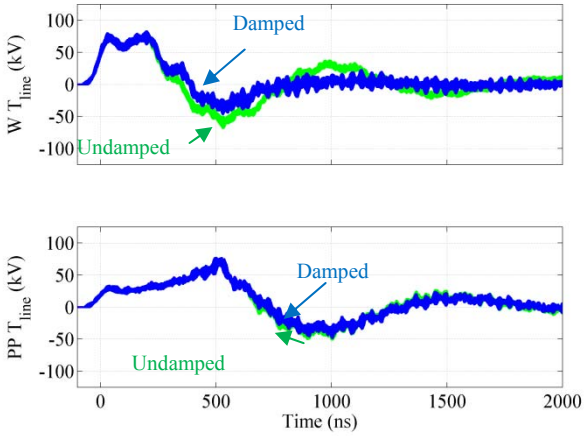

Figure 11. Transmission line voltages with fixed load inductance.

When utilizing active damping other components in the system can be stressed at higher levels. In particular, the switches, capacitors, and module interfaces. This is evident in Figure 12 where modules that are triggered late in time for damping have greater currents flowing through them because they are feeding the load and the other modules that have reversed polarity.

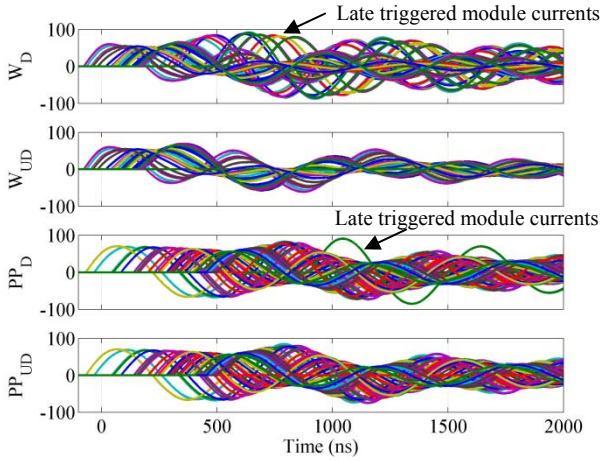

Figure 12. Module currents with fixed load inductance (D – damped, UD – undamped).

Once the simulated load current shapes have been determined using a fixed inductance the methods in Section III are employed to estimate the time varying load inductance specific to the given current shape. Figure 13 contains plots of the initial static inductance and the dynamic inductances estimated for the damped tungsten and polypropylene load current waveforms. From these estimates the inductance increases by over a factor of five at late times in the waveforms.

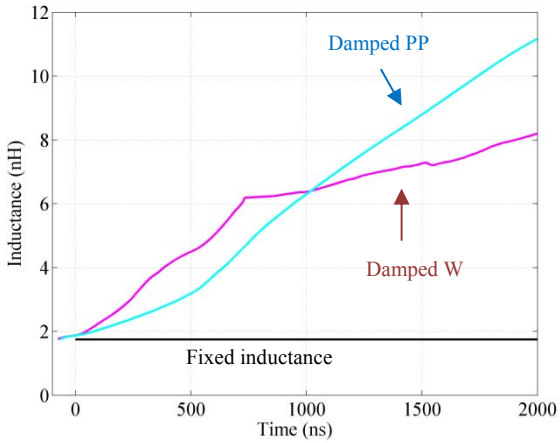

Figure 13. Static and dynamic load inductances for damped load current waveforms.

It must be kept in mind that the dynamic inductances in Figure 13 are only valid for specific load currents. Therefore to perform pulse shaping the simulations must be updated with the time varying inductance and new trigger times must be identified that result in the original simulated currents. An alternative technique to genetic optimization for choosing the trigger times was utilized in this next step. This technique approach is iterative, utilizes a fixed order to the triggering of the modules, and therefore only determines the trigger times that provide pulse shaping. The downside of this technique is that the

ability to minimize multiple constraints is lost. Future work will look at using genetic or other optimization approach for this next step in an attempt to minimize stresses in the system. Plotted in Figure 14 are the original fixed load inductance waveforms and the new dynamic load inductance waveforms. Early in time over the range of the ideal waveform good agreement is achieved. The tungsten waveform with dynamic loads used 180 modules up to 849 ns the remaining modules were triggered at 1993 ns. The polypropylene waveform with dynamic loads used 200 modules up to 489 ns, the remaining modules were triggered at 1249 ns causing the additional late time ringing.

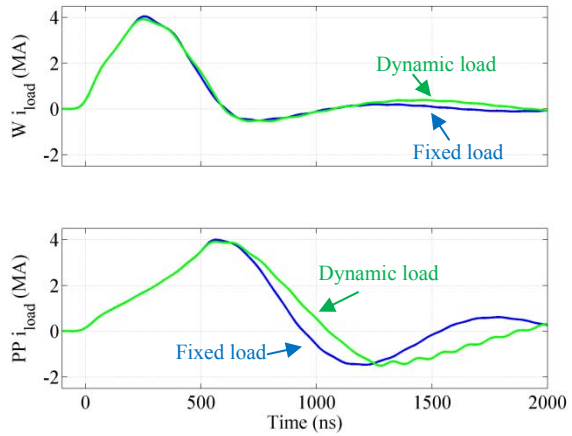

Figure 14. Load currents with dynamic load inductance, damped load current waveforms.

Increasing inductance does result in greater dielectric stresses in the transmission line plates as can be seen in Figure 15 where peak voltages that were significantly lower than 100 kV now reach and even exceed 100 kV. The effect is even greater when comparing the reversal voltages.

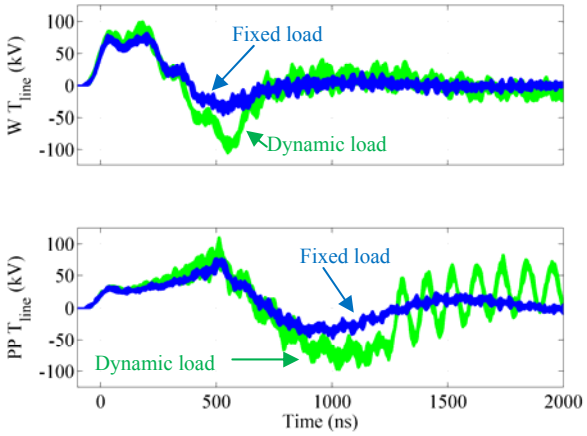

Figure 15. Transmission line voltages with dynamic load inductance, for damped load current waveforms.

Some module currents also increase in this simulation as shown in Figure 16. This is primarily due to the choice of trigger times and the larger transmission line plate voltage reversal that appears with the dynamic load. A multi-constraint optimization technique may help with some of this but connecting late time modules across the transmission line plate at a larger reversal point will impact the amplitude of module currents.

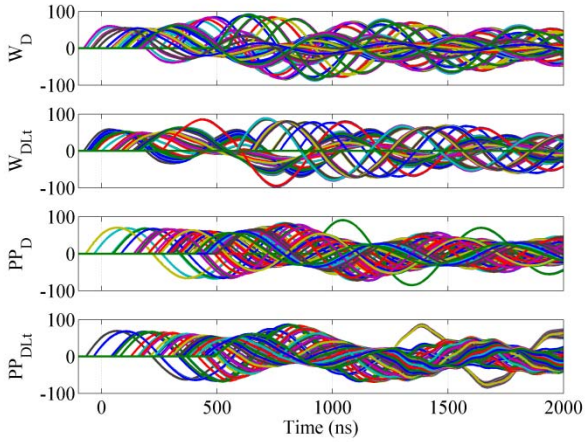

Figure 16. Module currents with dynamic load inductance, for damped load current waveforms (Lt – time varying load).

The analysis and simulation presented in this section demonstrate the flexibility and performance of the technologies being advanced for low impedance pulsed power current adders such as Genesis. Furthermore the requirement for high fidelity models becomes immediately apparent. Research continues to address these needs relative to both the time varying loads discussed in this paper and other critical system components, such as the switch, discussed in [11].

V. CONCLUSION

The dynamic behavior of the stripline and material sample which form the load for Genesis impacts the performance of this system in a complex manner. It is necessary to quantify this dynamic interaction in order to develop module triggering sequences which are capable of producing precision pressure profiles in a given target material. Given the broad operating range of Genesis, it is possible to identify optimal triggering sequences to account for dynamic interactions in various materials. It is also possible to shape pressure profiles while addressing system lifetime drivers such as late time ringing and peak disk plate peak voltage variations.

VI. ACKNOWLEDGEMENTS

The authors would like to thank: H.D. Anderson, H.L. Brown, M.L. Horry, M.D. Knudson, M.J. Madlener, G.

Neau, V. Romero, S.D. Sudhoff, and R. White for their support, insight, and valuable discussions regarding this project. The authors also gratefully acknowledge valuable contributions from their colleagues at Sandia National Laboratories, Ktech Corporation, EG&G, L-3 Communications, and Purdue University.

VII. REFERENCES

[1] L. K. Warne, R. S. Coats, R. E. Jorgenson, and W. A. Johnson, "Load Impedance and Current Distribution for Pulsed Power Device," Sandia National Laboratories Internal Report, December 19, 2007, LKWarne@sandia.gov.

[2] M.G. Mazarakis, et al., "High current, 0.5 MA, fast, 100ns linear transformer driver experiments," Physical Review Special Topics – Accelerators and Beams, 12, 050401 2009. .

[3] B.M. Kovalchuk, et al. "Multi gap switch for Marx generators," Pulsed Power Plasma Science Conference, June, 2001, pp. 1739-1742.

[4] J. R. Woodworth, et al., "Low-inductance gas switches for linear transformer drivers," Physical Review Special Topics – Accelerators and Beams 12, 060401, 2009.

[5] MATLAB The Language of Technical Computing, The MathWorks, Inc., 3 Apple Hill Drive, Natick, MA 01760-2098 USA, info@mathworks.com.

[6] S.F. Glover, et al., "Genetic optimization for pulsed power system configuration," IEEE Transactions on Plasma Science, Vol. 37, No. 2, February 2009, pp. 339-346.

[7] S.D. Sudhoff and Y. Lee, "Energy Systems Analysis Consortium (ESAC) Genetic Optimization System Engineering Tool, v. 2.2 Manual," School of Electrical and Computer Engineering., Purdue Univ., West Lafayette, IN., 47907. sudhoff@ecn.purdue.edu

[8] S.F. Glover, et al., "Genesis: A 5 MA programmable pulsed power driver for isentropic compression experiments," IEEE Transactions on Plasma Science, Vol. 38, No. 1, October, 2010, pp. 2620-2626.

[9] A. C. Robinson, et al., "ALEGRA: An Arbitrary Lagrangian-Eulerian Multimaterial, Multiphysics Code," AIAA 2008-1235, 46th AIAA Aerospace Sciences Meeting and Exhibit, 2008.

[10] R. W. Lemke, et al., "Characterization of magnetically accelerated flyer plates," *Physics of Plasmas*, Vol. 10, No. 4, April 2003, pp. 1092-1099.

[11] S.F. Glover, et al., "Status of Genesis a 5 MA programmable pulsed power driver," 18th IEEE International Pulsed Power Conference, June 2011.

REFERENCES BELOW THIS LINE ARE NOT REFERENCED

[12] C. A. Hall, "Isentropic compression experiments on the Sandia Z accelerator," Physics of Plasmas, Vol. 7, No. 5, May 2000, pp. 2069-2075.

[13] J.P. Davis, et al., "Magnetically driven isentropic compression to multimegabar pressures using shaped current pulses on the Z accelerator," Physics of Plasmas, vol. 12, no. 5, 2005.

[14] T. Ao, et al., "A compact strip-line pulsed power generator for isentropic compression experiments," Review of Scientific Instruments, 79, 013903, 2008.

[15] SolidWorks 3D CAD Software, Dassault Systèmes SolidWorks Corp., 300 Baker Avenue, Concord, MA 01742, USA, www.solidworks.com

[16] G. Neau, L3 Communications, 4855 Ruffner St., Suite A, San Diego, CA 92111.

[17] Jane Lehr, et al., "Evaluation of Spark Gap Switches Operated at Low Percent of Self Break Voltage," 17th IEEE Pulsed Power Conference, June 2009.

[18] S.F. Glover, et al., "Pulsed and DC Charged PCSS Based Trigger Generator," 17th IEEE Pulsed Power Conference, June 2009.

[19] S.F. Glover, et al., "Pulsed and DC charged PCSS based trigger generators," *IEEE Transactions on Plasma Science*, Vol. 38, No. 1, October, 2010, pp. 2701-2707.

[20] W. A. Stygar, et al,"Shaping the output pulse of a linear-transformer-driver module," Physical Review Special Topics – Accelerators and Beams, 12, 030402, March 2009.

Abstract # 1167, can be up to six pages (eight if it is an invited paper) THIS IS INVITED